

# Double-Peaked Broad Emission Lines and the Geometry of Accretion in AGNs

I. STRATEVA, M. A. STRAUSS, and L. HAO  
*Princeton University*

---

## Abstract

Although accretion disks are a theoretically appealing model for the geometry and dynamics of the gas in the vicinity of black holes in Active Galactic Nuclei (AGN), there is little direct observational evidence for their existence. The telltale signature of disk emission in AGN – *double peaked emission lines* – have so far been found in only two dozen cases in the optical ([1], [2]). We have selected  $\sim 100$  double-peaked broad emission line AGN from the Sloan Digital Sky Survey (SDSS) from a large sample of over 4000 AGN with  $z < 0.4$ . By comparing the properties of these AGN with those of the full sample, we hope to isolate the defining characteristics of disk-emitters and ultimately answer the question: “If all AGN have accretion disks, why don’t they all show double-peaked disk emission lines?” Here we present Gaussian parameterized  $H\alpha$  line-profile measurements for the sample of double-peaked AGN in comparison with circular and elliptical accretion disk models.

## 1.1 Introduction

Disk accretion provides a highly efficient mechanism for the dissipation of angular momentum, allowing for the conversion of large fraction of the rest-mass energy of the material accreted onto a black hole in the form of radiation. Because AGN are the most luminous compact sources observed, accretion disks are believed to be responsible for their continuum emission and the formation of jets. Mass-transferring binary systems, containing stellar mass black holes (*e.g.* low mass X-ray binaries) or other compact objects (*e.g.* white dwarfs in cataclysmic variables and dwarf novae), provide numerous examples of disk accretion. Extensive light-curve and time-lag (both continuum and emission-line) observations of these binary systems give conclusive evidence for the existence of accretion disks ([3], [4]), along with detailed temperature and surface density maps and striking examples of hot spots and spiral structures (*e.g.* IP Peg, [5]). The emission signatures of disks in AGN are much more elusive, owing to the impossibility of resolving the disk structures and following their time variation in even the nearest galactic nuclei. The complex interplay of disk radiation reprocessing in hot coronas, jets and winds, driven by the presence of multiphase plasma in the vicinity of the central engine, make it virtually impossible to compute the AGN spectral energy distribution from first principles, further frustrating the interpretation of observations.

Despite the complexity of the black hole environment, a small class of AGN do show the

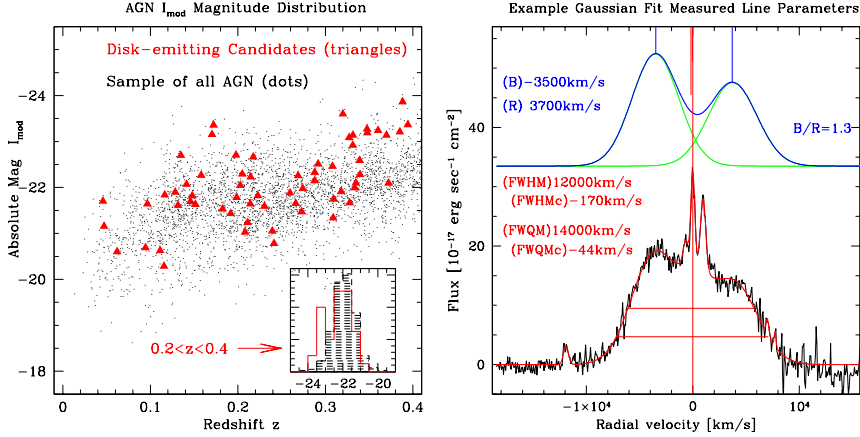


Fig. 1.1. *Left*: Absolute magnitude distribution of candidate disk-emitters (red) compared to that of the full AGN sample over the same redshift range (black). *Right*: Example Gaussian fit. The original profile is in black, the Gaussian fit overlaid in red. The blue line (displaced vertically) shows the fitted double-peaked  $H\alpha$  after subtraction of the narrow lines and a central broad  $H\alpha$  component.

double-peaked broad lines characteristic of disk emission in the optical. These AGN present us with a unique opportunity to study the structure of AGN accretion disks.

## 1.2 Data Analysis

The Sloan Digital Sky Survey ([6], [7]) will produce upon completion a catalog of over  $10^5$  multicolor selected AGN with five-band ( $ugriz$ ) photometry and calibrated spectra covering the wavelength region 3800–9200Å at a spectral resolution of 1850–2200. The identification and basic measurements for the sample are done automatically by a series of custom pipelines. The spectroscopic observations are carried out using the 2.5m SDSS telescope at Apache Point Observatory and a pair of double, fiber-fed spectrographs.

Using the SDSS spectroscopic survey we selected  $\sim 100$  double-peaked broad line AGN based on their  $H\alpha$  line profiles. The absolute magnitude distribution of the sample vs. redshift is presented in the left panel of Figure 1.1 in comparison with that of all AGN. In order to characterize the line profiles in a model-independent way, we subtract a sum of stellar + power law continua ([8]) and fit a sum of Gaussians to each  $H\alpha$  line complex (see the right panel of Figure 1.1 for an example). We use the resulting smooth Gaussian profiles to estimate the positions (in velocity space relative to the narrow  $H\alpha$  component) of the blue and red peaks, the blue-to-red peak ratio, the peak separation, the FWHM and the  $FW_{\frac{1}{4}M}$  (*i.e.*, measured at  $\frac{1}{4}$  maximum) of the broad line component and the displacements of their respective centroids. By comparing the distribution of these line-characterizing quantities with those measured on a set of accretion disk models, we find the distribution of disk model parameters that best describe the data in a statistical sense. For the present comparison we have chosen one axisymmetric (circular) accretion disk model with intrinsic turbulent broadening [9] and the simplest non-axisymmetric disk model, that of an elliptical disk [10].

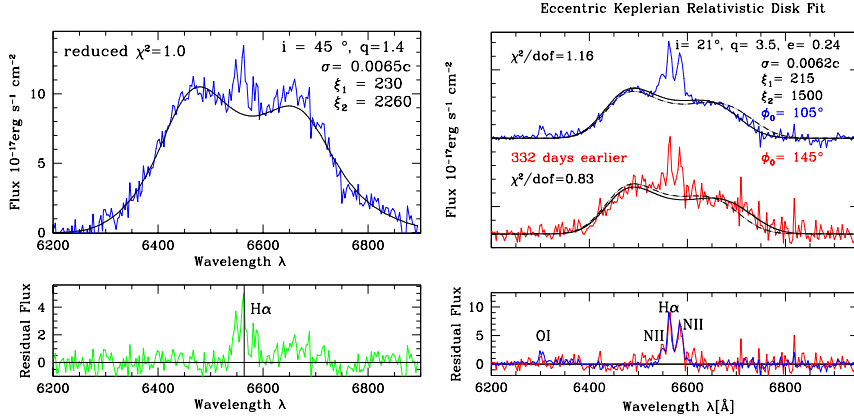


Fig. 1.2. *Left*: circular disk fit and model parameters (top) and residual narrow lines (bottom). *Right*: elliptical disk fits at two epochs (the red spectrum was observed one year before the blue; top) and narrow line residuals (bottom). The observed disk precession of  $\sim 40^\circ$  between the two epochs, implies a precession period of just over 8 years. The precession period,  $P_{GR}$ , is approximately  $P_{GR} \approx 2 \times M_7 (\xi/200)^{2.5}$  years ([1]), leaving us with a plausible black hole mass of  $\sim 2.5 \times 10^6 M_\odot$ . This is, of course, an over-interpretation of 2 epochs of data; the example is merely intended to be illustrative.

### 1.3 Accretion Disk Models

We created  $\sim 25,000$  model disk-emission line profiles for comparison with observations, by varying all model parameters on a grid. The circular disk model (after [9]) assumes a simple relativistic Keplerian disk which is geometrically thin and optically thick and has five parameters: the inner and outer radii of the emitting ring (in units of the gravitational radius,  $R_G = 2GM_\bullet/c^2$ ),  $\xi_1$  and  $\xi_2$ , the disk inclination,  $i$ , the slope of the surface emissivity power law,  $q$ , and the turbulent broadening,  $\sigma$ . These parameters correspond to the five parameters of a two-Gaussian fit representation of the double-peaked profile, *i.e.*, the model is fully constrained by the Gaussian fit. Doppler boosting of radiation results in a higher blue peak than red in the circular disk case, and a net redshift of the whole line is observed.

If the red peak is stronger than the blue, or the profile is observed to be variable in this sense, the circular disk emission profile model fails and some asymmetry in the disk has to be invoked to reproduce the line asymmetry. Common choices are elliptical disks (thought to arise when a single star is disrupted in the vicinity of a black hole, [10]), warped disks (theorized to exist around rotating black holes, [11]; spiral disks ([12], [13]), or disks with a hot spot ([14]). The choice of the elliptical disk to represent all non-axisymmetric disks in this comparison is justified solely by its relative simplicity and the fact that we do not have the extensive time variability observations required to distinguish between the different non-axisymmetric models. Example circular and elliptical disk fits are given in Figure 1.2. Note that a *statistical* comparison of the observed and disk-model line profiles, as the one we present here, is more meaningful in terms of characterizing the distribution of accretion disk parameters in AGN than individual kinematic profile fits, especially in view of the observed

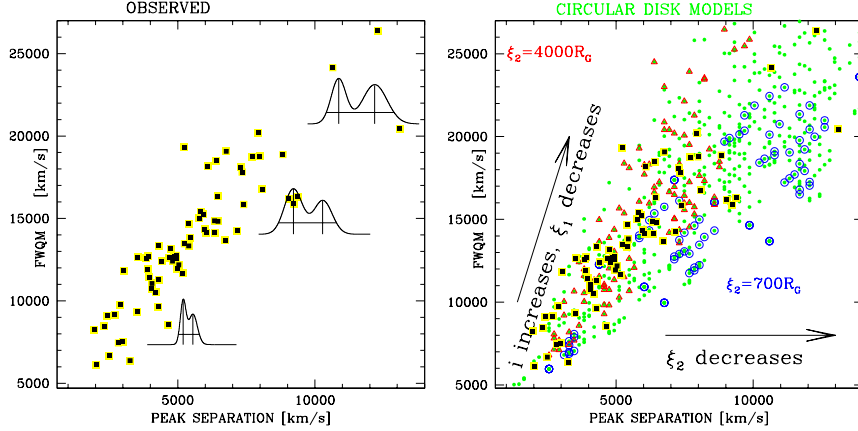


Fig. 1.3. *Left: Observed* peak separation vs.  $\text{FW}\frac{1}{4}\text{M}$  and 3 Gaussian fits for illustration. *Right: Circular disk models.* Each point corresponds to a double peak model realization. The inclination  $i$  (larger effect) and inner radius,  $\xi_1$ , determine the  $\text{FW}\frac{1}{4}\text{M}$ , while the peak separation is governed by the outer radius,  $\xi_2$ . The red triangles (blue circles) correspond to models with largest (smallest) outer radii.

frequent variability of the line profiles. Individual model fits will be presented in a follow up paper.

#### 1.4 Statistical Comparison of Disk-Model and Observed Line Profiles

The left panel of Figure 1.3 presents the observed peak separation vs. the  $\text{FW}\frac{1}{4}\text{M}$  of the emission line which we compare to a select subset of circular disk models in the right panel. The  $\text{FW}\frac{1}{4}\text{M}$  of a model line profile increases most strongly with increasing disk inclination,  $i$ , and also with decreasing inner radius of the emitting region,  $\xi_1$ , while the peak separation increases with decreasing outer radius,  $\xi_2$ . The current sample of disk emitters is consistent with accretion disks with inclinations  $15^\circ < i < 45^\circ$ , inner radii of  $200R_G < \xi_1 < 600R_G$  and outer radii of  $1500R_G < \xi_2 < 4000R_G$ . Emission lines produced in disks of smaller inclinations are single-peaked, and thus not selected from the observed data for this comparison. There is no *a priori* reason why we should not observe disks at higher inclinations, so the lack of such observed profiles could be telling us that we are looking through the dusty torus believed to exist at larger radii in unified models of AGN. By comparing the position of the FWHM centroid of the observed line profiles and the disk models, we conclude that at least half of the cases require non-axisymmetric disks. The results of this comparison are illustrated in the right panel of Figure 1.4.

#### 1.5 Conclusions

Further exploration of the physical conditions of the disk through kinematic modeling of the individual line profiles, combined with flux measurements in different wavebands, and complemented by variability and spectropolarimetric observations will eventually help us sketch the geometry of accretion in these objects, while comparison of the properties of these select AGN with the rest of the sample allows us to address the question of the lack of obvious disk emission in the full AGN sample. Such statistical studies were impossible on

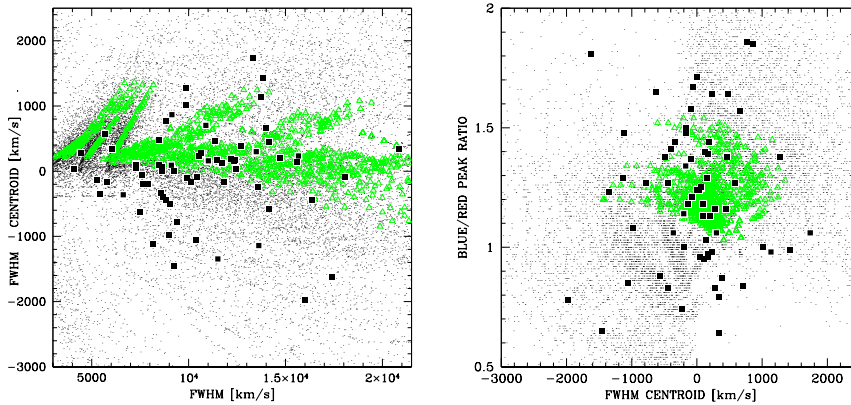


Fig. 1.4. **Observed vs. model comparison suggests the need for non-axisymmetric disks.** Black squares stand for observed quantities, green triangles for axisymmetric (circular) disk models, and black dots for non-axisymmetric (elliptical) models. *Left:* FWHM vs. FWHM centroid. *Right:* Peaks centroid vs. Blue/Red peak height ratio.

the basis of the small samples existing before. The current SDSS sample is  $\sim 4$  times larger than previous samples (*e.g.*, [1], [2]) and will increase twofold by the survey end.

**Acknowledgments.** We would like to thank Michael Eracleous, Pat Hall, Li-Xin Li, Wei Zheng, and Bohdan Paczynski for their guidance and useful discussions. Funding for the SDSS is provided by the Alfred P. Sloan Foundation, NASA, NSF, DoE, Monbukagakusho, the Max Planck Society and the member institutions.

## References

- [1] Eracleous, M. 1999, in Structure and Kinematics of Quasar Broad-Line Regions, ed. C. M. Gaskell et al. (San Francisco: ASP), 163
- [2] Eracleous, M. & Halpern, J. P. 1994, ApJS, 90, 1
- [3] Harlaftis, E. T. 2000, astro-ph/0012513
- [4] Vriellmann, S. 2000, astro-ph/0012263
- [5] Steeghs, D., Harlaftis, E. T., & Horne, K. 1997, MNRAS, 290, L28
- [6] York, D. G., et al. 2000, AJ, 120, 1579
- [7] Gunn, J.E., et al. 1998, AJ, 116, 3040
- [8] Hao, L., & Strauss, M. A. 2003, Carnegie Observatories Astrophysics Series, Vol. 1: Coevolution of Black Holes and Galaxies, ed. L. C. Ho (Pasadena: Carnegie Observatories, <http://www.ociw.edu/ociw/symposia/series/symposium1/proceedings.html>)
- [9] Chen, K., & Halpern, J. P. 1989, ApJ, 344, 115
- [10] Eracleous, M., Livio, M., Halpern, J. P., & Storchi-Bergmann, T. 1995, ApJ, 438, 610
- [11] Hartnoll, S. A., & Blackman, E. G. 2000, MNRAS, 317, 880
- [12] Chakrabarti, S. K., & Wiita, P. J. 1994, ApJ, 434, 518
- [13] Hartnoll, S. A., & Blackman, E. G. 2002, MNRAS, 332, L1
- [14] Zheng, W., Veilleux, S., & Grandi, S. A. 1991, ApJ, 381, 418